JAIST Repository
https://dspace.jaist.ac.jp/

Title	Theoretical Assessment of FePt Nanoparticles as Heating Elements for Magnetic Hyperthermia
Author(s)	Maenosono, Shinya; Saita, Soichiro
Citation	IEEE Transactions on Magnetics, 42(6): 1638-1642
Issue Date	2006-06
Type	Journal Article
Text version	publisher
URL	http://hdl.handle.net/10119/4654
Rights	Copyright (c)2006 IEEE. Reprinted from IEEE Transactions on Magnetics , 42(6), 2006, 1638-1642. This material is posted here with permission of the IEEE. Such permission of the IEEE does not in any way imply IEEE endorsement of any of JAIST's products or services. Internal or personal use of this material is permitted. However, permission to reprint/republish this material for advertising or promotional purposes or for creating new collective works for resale or redistribution must be obtained from the IEEE by writing to pubs-permissions@ieee.org. By choosing to view this document, you agree to all provisions of the copyright laws protecting it.
Description	

JAIST
JAPAN
ADVANCED INSTITUTE OF
SCIENCE AND TECHNOLOGY

Japan Advanced Institute of Science and Technology

Theoretical Assessment of FePt Nanoparticles as Heating Elements for Magnetic Hyperthermia

Shinya Maenosono[1] and Soichiro Saita[2]

[1]Department of Chemical System Engineering, University of Tokyo, Tokyo 113-8656, Japan
[2]Mitsubishi Chemical Group Science and Technology Research Center Inc., Kanagawa 227-8502, Japan

FePt magnetic nanoparticles (MNPs) are expected to be a high-performance nanoheater for magnetic hyperthermia because of their high Curie temperature, high saturation magnetization, and high chemical stability. Here, we present a theoretical performance assessment of chemically disordered fcc-phase FePt MNPs. We calculate heat generation and heat transfer in the tissue when an MNP-loaded tumor is placed on an external alternating magnetic field. For comparison, we estimate the performances of magnetite, maghemite, FeCo, and $L1_0$-phase FePt MNPs. We find that an fcc FePt MNP has a superior ability in magnetic hyperthermia.

Index Terms—**Bioheat transfer equation, cancer treatment, hyperthermia, iron-platinum nanoparticle.**

I. Introduction

HYPERTHERMIA is one of many techniques used in oncology, based on heating tumors for therapeutic purposes, and usually used as an additive therapy with standard treatments, such as radiotherapy and chemotherapy. The principle of cancer treatment is to eliminate only cancer cells distinguishing from normal cells. They are distinguished by visual inspection in surgical procedure. However, cellular discrimination is difficult. Although various efforts have been made to attain tumor-selective radiotherapy and chemotherapy, there remains considerable difficulty in these techniques. Hyperthermia is superior to other therapeutic techniques on this point. The blood flow is insufficient in tumors and the inadequate blood flow makes tumors more acidic due to the lactic acid buildup in the tumor tissues from lack of oxygen. In general, cells are easy to die when the environment becomes acidic, because temperature-sensitivity of cell increases. Additionally, the temperature will rise easily when the blood flow is insufficient. Moreover, cancer cells have a lower thermal resistance than normal cells. In consequence, one can eliminate cancer cells selectively by rising the local temperature at the site of tumor.

The magneto-thermo-cytolysis (or the magneto-thermoablation) is a promising technique thanks to the development of precise methods for synthesizing functionalized magnetic nanoparticles (MNPs) [1]. MNPs with functionalized surfaces, which have high specificity to a tumor tissue, are used as heating elements for hyperthermia. The process involved in the magnetic hyperthermia is based on the energy dissipation when a ferromagnetic material is placed on an external alternating magnetic field. The energy dissipation of MNPs consists of the following two effects: the Néel relaxation and the Brownian relaxation. For efficient magnetic hyperthermia, the MNPs are required to have low toxicity and a high saturation magnetization in order to minimize the doses needed for temperature increase.

In this context, iron-platinum (FePt) nanoparticle is a promising candidate because presents a high Curie temperature, high saturation magnetization, and high chemical stability [2]. Recently, a colloid-chemical synthesis technique of FePt MNPs has been developed and the FePt MNPs are regarded as one of the most likely candidates for ultrahigh-density nano-sized magnetic recording materials [2][3]. The colloid-chemically synthesized FePt MNPs have chemically disordered face-centered cubic (fcc) structure in which Fe and Pt atoms are randomly arranged and are superparamagnetic. Post-synthesis thermal annealing at a temperature over 580 °C transforms the crystalline structure from fcc to chemically ordered $L1_0$ phase. $L1_0$-phase FePt MNPs have a large magnetocrystalline anisotropy ($K = 7 \times 10^6$ J/m^3) [4], and thus exhibit large coercivity at room temperature, even when their size is as small as several nanometers. For bio applications such as heating elements for hyperthermia, however, a superparamagnetic fcc-phase FePt MNP is also an attractive material. For this purpose, it is important to know the targeted value of MNP size, because the mean size control attaining desirable average composition and uniformity of FePt MNPs is still a big challenge. Chen *et al.* have synthesized FePt MNPs of average diameter with a size of up to 9 nm by precisely controlling reaction conditions, such as the kind of solvent used, the amount of capping agents, temperature, temperature rising rate, and reaction time [5]. However, in general, it is difficult to synthesize FePt MNPs of average diameter that are larger than 5 nm with uniform size and composition distributions. Here, we theoretically considered an applicability of FePt MNPs to magnetic hyperthermia comparing with iron oxide and permendur MNPs, and clarified the requirements for the synthesis of FePt MNPs when one applies FePt MNPs as heating elements for hyperthermia.

II. Theory

The energy dissipation of MNPs in an alternating magnetic field is described as [6]

$$P = \pi \mu_0 \chi_0 H_0^2 f \frac{2\pi f\tau}{1 + (2\pi f\tau)^2} \tag{1}$$

where μ_0 is the permeability of free space, $4\pi \times 10^{-7}$ T·m/A; χ_0 is the equilibrium susceptibility; H_0 and f are the amplitude and

Digital Object Identifier 10.1109/TMAG.2006.872198

0018-9464/$20.00 © 2006 IEEE

the frequency of alternating magnetic field; and τ is the effective relaxation time given by

$$\tau^{-1} = \tau_{\mathrm{N}}^{-1} + \tau_{\mathrm{B}}^{-1} \tag{2}$$

where τ_{N} and τ_{B} are the Néel relaxation and the Brownian relaxation time, respectively. τ_{N} and τ_{B} are written as

$$\tau_{\mathrm{N}} = \frac{\sqrt{\pi}}{2}\tau_0 \frac{\exp(\Gamma)}{\sqrt{\Gamma}} \tag{3}$$

$$\tau_{\mathrm{B}} = \frac{3\eta V_{\mathrm{H}}}{kT} \tag{4}$$

where τ_0 is the average relaxation time in response to a thermal fluctuation; η is the viscosity of medium; V_{H} is the hydrodynamic volume of MNP; k is the Boltzmann constant, 1.38×10^{-23} J/K; T is the temperature. Here, $\Gamma = KV_{\mathrm{M}}/kT$ and V_{M} is the volume of MNP. The MNP volume V_{M} and the hydrodynamic volume including the ligand layer V_{H} are written as

$$V_{\mathrm{M}} = \frac{\pi D^3}{6} \tag{5}$$

$$V_{\mathrm{H}} = \frac{\pi(D+2\delta)^3}{6} \tag{6}$$

where D is the diameter of MNP; δ is the ligand layer thickness. The equilibrium susceptibility χ_0 is assumed to be the chord susceptibility corresponding to the Langevin equation, and expressed as

$$\chi_0 = \chi_{\mathrm{i}} \frac{3}{\xi}\left(\coth\xi - \frac{1}{\xi}\right) \tag{7}$$

where $\xi = \mu_0 M_{\mathrm{d}} H V_{\mathrm{M}}/kT; M_{\mathrm{S}} = \phi M_{\mathrm{d}}; H = H_0 \cos 2\pi ft$; and ϕ is the volume fraction of MNPs. Here, M_{d} and M_{S} are the domain and saturation magnetization, respectively. The initial susceptibility is given by $\chi_{\mathrm{i}} = \mu_0 \phi M_{\mathrm{d}}^2 V_{\mathrm{M}}/3kT$. The temperature rise is calculated as $\Delta T = P\Delta t/\rho c_{\mathrm{p}}$ where ρ and c_{p} are the effective density and the effective specific heat calculated as $\rho = \phi\rho_1 + (1-\phi)\rho_2$ and $c_{\mathrm{p}} = \phi c_{\mathrm{p1}} + (1-\phi)c_{\mathrm{p2}}$, where subscripts 1 and 2 represent the MNPs and the medium, respectively.

III. Heating Rate of Aqueous Dispersions of MNPs

Based on the above-mentioned theory, we calculated the rate of temperature rise for aqueous dispersion of monodispersed equiatomic fcc-phase FePt MNPs varying the diameter of MNP (D) in adiabatic condition. For comparison, we also estimated the rates of temperature rise for magnetite (Fe_3O_4), maghemite (γ-Fe_2O_3), permendur (FeCo) and $L1_0$-phase FePt MNPs. In Table I, physical properties of each magnetic material are shown. The magnetocrystalline anisotropy constant (K) of fcc-phase FePt MNPs is estimated by using the relation $K = 25kT_{\mathrm{B}}/V_{\mathrm{M}}$, where T_{B} denotes the blocking temperature [7]. The temperature-dependent magnetization measurements of 4-nm fcc-phase FePt particles indicated that superparamagnetic behavior was blocked at 20 to 30 K [2]. Hence, we estimated as $K \cong 2.06 \times 10^5$ J/m^3 for fcc-phase FePt MNPs by setting $T_{\mathrm{B}} = 20$ K. The domain magnetization M_{d} of FePt [8] and FeCo [9] MNPs are estimated by using bulk values of M_{S}. The surface dead layer effect [10] and polydispersity of MNPs are not considered in our calculations. In practice, the magnetic anisotropy may vary considerably due to the shape contributions of MNPs. For simplicity, however, the shape effect is not taken into account in the present model. It has been pointed out that hysteresis losses are important especially for magnetic single domain particles with high magnetocrystalline anisotropy [11]. However, the hysteresis losses are not considered, because we assume MNPs are superparamagnetic in this study.

TABLE I
Physical Properties and Most Operative Sizes

Material	M_{d} kA/m	K kJ/m^3	c_{p} J/(kg·K)	ρ kg/m^3	$D_{\max}$ [k] nm
Magnetite	446 [a]	9 [d]	670 [a]	5180	19
Maghemite	414 [a]	4.7 [e]	746 [a]	4600	23.5
FeCo	1790 [b]	1.5 [f]	172 [i]	8140	34
fcc FePt	1140 [c]	206 [g]	327 [j]	15200	9
$L1_0$ FePt	1140 [c]	7000 [h]	295 [j]	15200	9

[a][6], [b][9], [c][8], [d][12], [e][13], [f][14], [g]Estimated by K=25$kT_{\mathrm{B}}/V_{\mathrm{M}}$, [h][4], [i][15], [j][16], [k]H_0=50 mT and f=300 kHz.

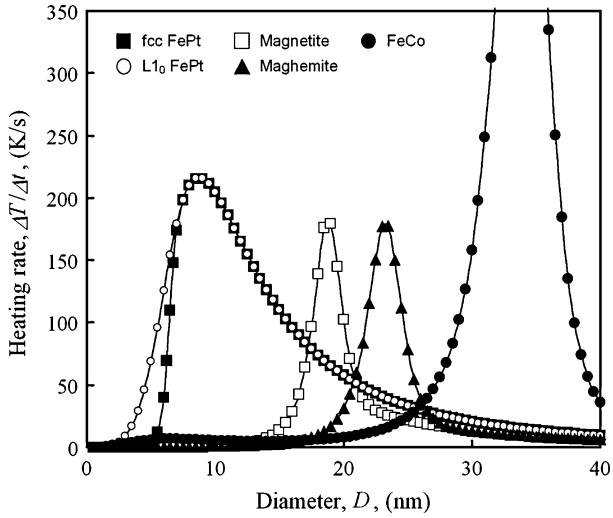

Fig. 1. Comparative heating rates as a function of particle diameter for various MNPs. Filled squares and open circles represent fcc- and $L1_0$-phase FePt, respectively. Open squares and filled triangles are magnetite and maghemite, respectively. Filled circles represent FeCo MNPs. $H_0 = 50$ mT and $f = 300$ kHz.

Fig. 1 shows comparative heating rates for aqueous monodispersions of the various MNPs listed in Table I, assuming $\tau_0 = 10^{-9}$ s and $\phi = 0.1$. Amplitude and frequency of applied magnetic field were fixed at 50 mT and 300 kHz. The carrier liquid is pure water in all cases. Surface ligand layer thickness is assumed to be $\delta = 1$ nm. On these conditions, fcc- and $L1_0$-phase FePt MNPs yield the largest heating rates in the size range of $D < 20$ nm. Most operative sizes of each MNPs, $D_{\max}$, which give a maximum heating rate, are 9 nm for fcc- and $L1_0$-phase

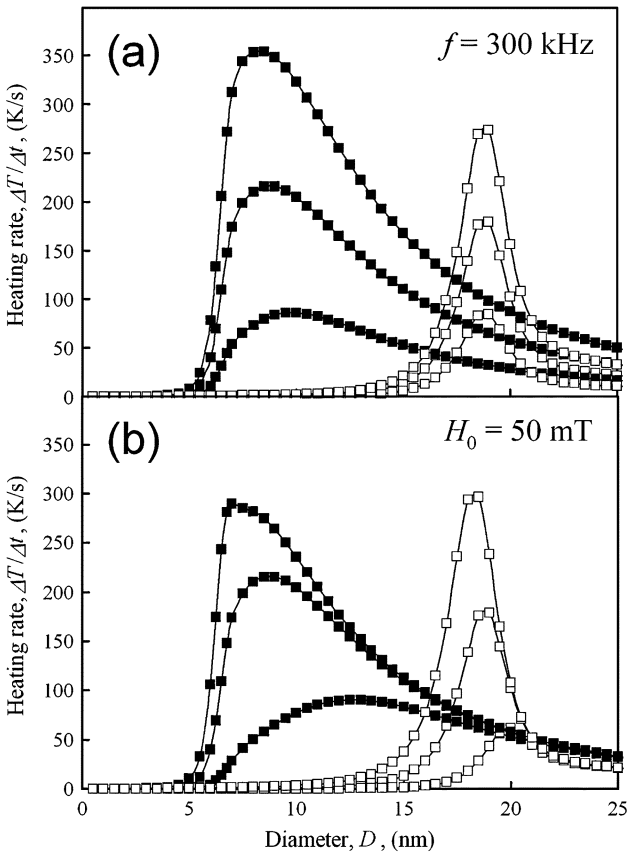

Fig. 2. (a) Dependence of heating rates on H_0. By fixing $f = 300$ kHz, H_0 is varied as 25 (bottom curve), 50 (middle) and 75 (top) mT. (b) Dependence of heating rates on f. By fixing $H_0 = 50$ mT, f is varied as 100 (bottom curve), 300 (middle) and 500 (top) kHz. Filled and open squares represent the cases of fcc FePt and magnetite MNPs, respectively.

FePt MNPs, 19 nm for magnetite, 23.5 nm for maghemite, and 34 nm for FeCo MNPs (Table I). The FeCo MNPs have the highest heating rates as shown in Fig. 1. The maghemite MNPs also have large heating rates as well as magnetite MNPs. However, the size ranges of FeCo and maghemite, where the heating is possible, are much larger than the typical size ranges of standard ferrofluids ($D = 8$–10 nm). In general, the stability of magnetic colloid becomes impaired when $D > 20$ nm due to the spontaneous magnetization. On the other hand, it is difficult to obtain independently isolated $L1_0$-phase FePt MNPs at this moment. Considering above-mentioned problems and other things such as chemical stability, we will focus on fcc FePt and magnetite MNPs hereafter.

Fig. 2(a) shows the dependence of heating rates on amplitude of applied magnetic field fixing $f = 300$ kHz. Note that H_0 is varied as 25, 50, and 75 mT, and only the cases of fcc FePt and magnetite MNPs are plotted. The heating rates simply increase with increasing H_0. In the case of fcc FePt MNPs, the increase in the heating rates is more prominent than that in the case of magnetite MNPs when H_0 increases. No change in $D_{\max}$ is observed for both MNPs. Fig. 2(b) shows the dependence of heating rates on f fixing $H_0 = 50$ mT. Note that f is varied as 100, 300, and 500 kHz. The heating rates increase with increasing f. Unlike in the case of Fig. 2(a), the heating rates of

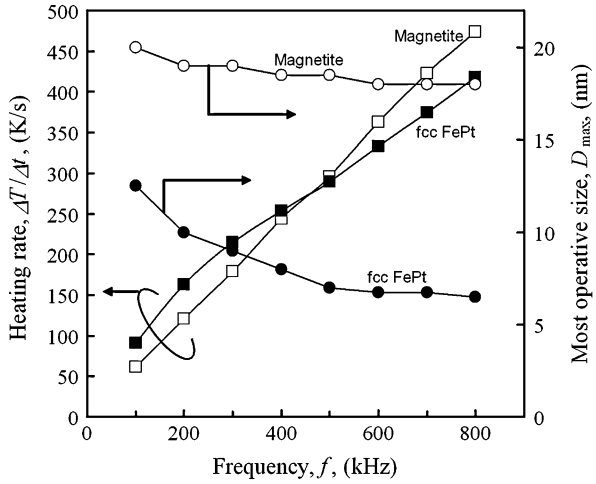

Fig. 3. Maximum heating rates (MHR) and $D_{\max}$ plotted as a function of f. Filled and open squares represent MHR of fcc FePt and magnetite, respectively. Filled and open circles are $D_{\max}$ of fcc FePt and magnetite, respectively.

magnetite MNPs increase with increasing f much faster than those of fcc FePt MNPs. The gradual decrease in $D_{\max}$ with increasing f is also observed for both MNPs.

In Fig. 3, the dependences of the maximum heating rates (MHR) and $D_{\max}$ on f ($f < 1$ MHz) for fcc FePt and magnetite MNPs are shown. The MHR of both MNPs linearly increase with increasing f. At low frequency range ($f < 500$ kHz), the MHR of fcc FePt MNPs are larger than those of magnetite MNPs as shown in Fig. 3. On the contrary, the MHR of magnetite MNPs are larger than those of fcc FePt MNPs when $f > 500$ kHz. On the other hand, $D_{\max}$ of fcc FePt MNPs decreases with increasing f, while that of magnetite MNPs does not change much. Thus, in the low frequency region ($f < 500$ kHz), fcc FePt MNPs have an advantage that they can heat tumors to higher temperatures than magnetite MNPs. At the high frequency range ($f > 500$ kHz), $D_{\max}$ of fcc FePt MNPs is quite smaller than that of magnetite MNPs. The saturation value of $D_{\max}$ of fcc FePt MNPs is 6 nm. This result indicates that the accumulation of MNPs in the tumor could be enhanced, because the specific surface area of FePt MNPs increases when the size of MNPs decreases, and thus, the specificity to a tumor tissue increases. Hence, the fcc FePt MNPs might have an advantage that the higher volume fraction of MNPs in the tumor tissue than that of magnetite MNPs can be attained. Consequently, the superiority of fcc FePt MNPs over the magnetite MNPs in hyperthermia is found to be prominent when H_0 is high and f is low.

IV. Bioheat Transfer Model

Several attempts to estimate the spatial temperature distribution in localized magnetic hyperthermia using MNPs have been reported. For example, Andrä *et al.* calculated the spatial temperature distribution in breast carcinomas containing magnetic particles under external alternating magnetic field by modified heat conduction equations [17]. They compared the calculated results with *in vitro* measurements with muscle tissue, and found a good agreement between the calculation and the experimental

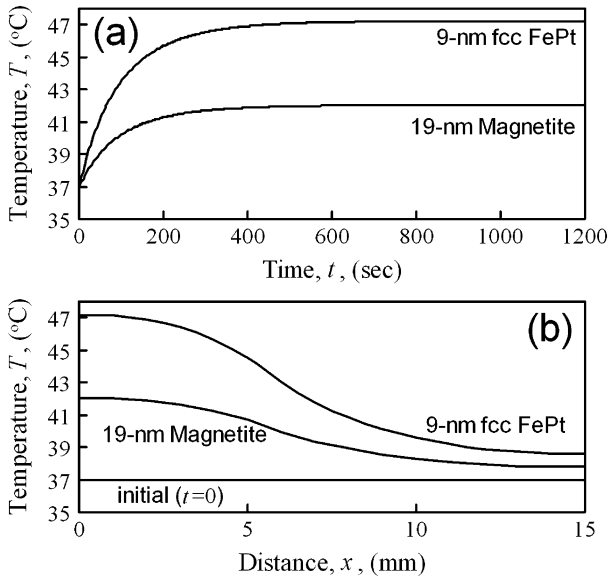

Fig. 4. (a) Time evolution of temperature at the center of the tumor ($H_0 = 50$ mT, $f = 300$ kHz, and $\phi = 2 \times 10^{-5}$). (b) Temperature distributions after applying external alternating magnetic field for 600 s. The interface between the tumor and normal tissue is located at $x = 5$ mm.

results. To estimate the temperature rise behavior *in vivo*, we solved the Pennes bioheat transfer equation [18] given by

$$\rho c_{\rm p} \frac{\partial T}{\partial t} = \nabla \kappa \nabla T + \rho_{\rm b} c_{\rm pb} \omega_{\rm b} (T_{\rm a} - T) + Q_{\rm met} + P \qquad (8)$$

where κ is the thermal conductivity of tissue, 0.502 W/(m · K) [19], [20]; $\rho_{\rm b}$ is the density of blood, 1000 kg/m^3 [21]–[24]; $c_{\rm pb}$ is the specific heat of blood, 4180 J/(kg · K) [21]–[24]; $\omega_{\rm b}$ is the blood perfusion rate, 6.4×10^{-3} s^{-1} [21]; $T_{\rm a}$ is the temperature of arterial blood, 310 K; and $Q_{\rm met}$ is the metabolic heat generation, 540 W/m^3. The effective density ρ and the effective specific heat $c_{\rm p}$ of the MNP-loaded tumor are given as the volume average as mentioned above, setting $\phi = 2 \times 10^{-5}$, $\rho_2 = 1060$ kg/m^3 [19], [22]–[24], and $c_{\rm p2} = 3600$ J/(kg · K) [19], [22]–[24]. By assuming a spherical tumor of 1 cm in diameter existing in the body core, we solved the one-dimensional form of (8) with the Neuman boundary conditions.

Fig. 4(a) shows the time evolution of temperature at the center of the tumor $(x = 0)$ in the cases of 9-nm fcc FePt and 19-nm magnetite MNPs ($H_0 = 50$ mT and $f = 300$ kHz). The energy dissipation is $P = 3.97 \times 10^5$ W/m^3 for fcc FePt MNPs and $P = 1.95 \times 10^5$ W/m^3 for magnetite MNPs. In general, cancer cells have a higher chance of dying when the temperature is above 42.5 °C, and the rate of death drastically increases with increasing temperature [25]. Hence, fcc FePt MNPs work well while magnetite MNPs do not in these conditions. This result indicates that one can significantly reduce the doses of MNPs producing the same effect. In practice, the MNPs in tumor tissue are considered to be immobilized in cell plasma or sticking on cell membranes. Therefore, the Brown relaxation pathway is thought to be nearly irrelevant. To consider this effect, we increased the medium viscosity η from the viscosity of water, and checked the changes in P for both MNPs. In the case of magnetite MNPs, P is independent of η, because the Néel relaxation dominates the relaxation process originally. On the other hand, P decreases with increasing η in the case of fcc FePt MNPs. However, P becomes to be independent of η when η increases more than 10 times the water viscosity. In such case, the value of P is 70% of original value. Even in this situation, the energy dissipation of fcc FePt MNPs is larger than that of magnetite MNPs.

Fig. 4(b) shows the steady-state temperature distributions after applying external alternating magnetic field of $H_0 = 50$ mT and $f = 300$ kHz for 600 s. The distance from the center of the tumor is represented as x. The interface between the tumor and normal tissue is located at $x = 5$ mm. As seen in Fig. 4(b), the range where the temperature is higher than 42.5 °C is $0 \leq x \leq 6$ mm. This indicates that the magnetic hyperthermia is highly selective for cancer treatments. Although the biocompatibility and cytotoxicity of FePt MNPs are still unclear at this moment, they are known to strongly depend on the kinds of surface capping molecules [26]. Hence, we do not elaborate on the biocompatibility and toxicity of FePt MNPs in the present paper.

V. Conclusion

Theoretical assessment of chemically disordered fcc-phase FePt MNPs as heating elements for magnetic hyperthermia is carried out by combining the heat generation model and the bioheat transfer equation. In consequence, fcc FePt MNPs are found to have a superior heating capability compared with other MNPs such as magnetite. Thus, significant reduction of the doses of MNPs is expected. However, one needs to synthesize larger FePt MNPs than 6 nm for their use in hyperthermia.

Acknowledgment

The authors would like to thank Dr. H. Asatani (Solid/Powder Processing Laboratory, MCRC, Inc.) for his helpful discussion.

References

[1] T. Neuberger, B. Schöpf, H. Hofmann, M. Hofmann, and B. von Rechenberga, "Superparamagnetic nanoparticles for biomedical applications: Possibilities and limitations of a new drug delivery system," *J. Magn. Magn. Mater.*, vol. 293, p. 483, 2005.

[2] S. Sun, C. B. Murray, D. Weller, L. Folks, and A. Moser, "Monodisperse FePt nanoparticles and ferromagnetic FePt nanocrystal superlattices," *Science*, vol. 287, p. 1989, 2000.

[3] S. Saita and S. Maenosono, "FePt nanoparticles with a narrow composition distribution synthesized via pyrolysis of iron(III) ethoxide and platinum(II) acetylacetonate," *Chem. Mater.*, vol. 17, p. 3705, 2005.

[4] K. Inomata, T. Sawa, and S. Hashimoto, "Effect of large Boron additions to magnetically hard Fe-Pt alloys," *J. Appl. Phys.*, vol. 64, p. 2537, 1988.

[5] M. Chen, J. P. Liu, and S. Sun, "One-step synthesis of FePt nanoparticles with tunable size," *J. Amer. Chem. Soc.*, vol. 126, p. 8394, 2004.

[6] R. E. Rosensweig, "Heating magnetic fluid with alternating magnetic field," *J. Magn. Magn. Mater.*, vol. 252, p. 370, 2002.

[7] V. Franco and A. Conde, "Influence of anisotropy on the grain size distribution derived from superparamagnetic magnetization curves," *J. Magn. Magn. Mater.*, vol. 277, p. 181, 2004.

[8] T. Klemmer, D. Hoydick, H. Okumura, B. Zhang, and W. A. Soffa, "Magnetic hardning and coercivity mechanisms in L1(0) ordered FePd ferromagnets," *Scr. Metall. Mater.*, vol. 33, p. 1793, 1995.

[9] C. Desvaux, C. Amiens, P. Fejes, P. Renaud, M. Respaud, P. Lecante, E. Snoeck, and B. Chaudret, "Multimillimeter-large superlattices of air-stable iron—cobalt nanoparticles," *Nature Mater.*, vol. 4, p. 750, 2005.

[10] X. W. Wu, C. Liu, L. Li, P. Jones, R. W. Chantrell, and D. Weller, "Nonmagnetic shell in surfactant-coated FePt nanoparticles," *J. Appl. Phys.*, vol. 95, p. 6810, 2004.
[11] R. Hergt, W. Andrä, C. G. d'Ambly, I. Hilger, W. A. Kaiser, U. Richter, and H.-G. Schmidt, "Physical limits of hyperthermia using magnetite fine particles," *IEEE Trans. Magn.*, vol. 34, no. 5, pp. 3745–3754 , Sep. 1998.
[12] R. C. O'Handley, *Modern Magnetic Materials*. New York: Wiley, 2000.
[13] J. K. Vassiliou, V. Mehrotra, M. W. Russell, E. P. Giannelis, R. D. McMichael, R. D. Shull, and R. F. Ziolo, "Magnetic and optical-properties of gamma-Fe_2O_3 nanocrystals," *J. Appl. Phys.*, vol. 73, p. 5109, 1993.
[14] R. V. Major and C. M. Orrock, "High saturation ternary cobalt-iron based alloys," *IEEE Trans. Magn.*, vol. 24, no. 2, pp. 1856–1858 , Mar. 1988.
[15] R. Kuentzler, "Low-temperature specific-heat of ordered and disordered FeCo," *Phys. Stat. Sol. B*, vol. 58, p. 519, 1973.
[16] G. Hausch, "High-temperature specific-heat of FeNi and FePt invar-alloys," *J. Magn. Magn. Mater.*, vol. 92, p. 87, 1990.
[17] W. Andrä, C. G. d'Ambly, R. Hergt, I. Hilger, and W. A. Kaiser, "Temperature distribution as function of time around a small spherical heat source of local magnetic hyperthermia," *J. Magn. Magn. Mater.*, vol. 194, p. 197, 1999.
[18] H. H. Pennes, "Analysis of tissue and arterial blood temperatures in the resting human forearm," *J. Appl. Physiol.*, vol. 1, p. 93, 1948.
[19] F. Duck, *Physical Properties of Tissue: A Comprehensive Reference Book*. New York: Academic, 1990, pp. 167–223.
[20] H. F. Bowman, , Shitzer and Eberhart, Eds., "Estimation of tissue blood flow," in *Heat Transfer in Medicine and Biology*. New York: Plenum, 1985, pp. 193–230.
[21] S. Tungjitkusolmun, S. T. Staelin, D. Haemmerich, J. Z. Tsai, J. G. Webster, F. T. Lee, D. M. Mahvi, and V. R. Vorperian, "Three dimensional finite element analyses for radio-frequency hepatic tumor ablation," *IEEE Trans. Biomed. Eng.*, vol. 49, no. 1, pp. 3–9, Jan. 2002.
[22] L. A. Geddes and L. E. Baker, "The specific resistance of biological material—A compendium of data for the biomedical engineer and physiologist," *Med. Biol. Eng.*, vol. 5, p. 271, 1967.
[23] O. P. Gandhi, G. Lazzi, and C. M. Furse, "Electromagnetic absorption in the human head and neck for mobile telephones at 835 and 1900 MHz," *IEEE Trans. Microw. Theory Tech.*, vol. 44, no. 10, pp. 1884–1897, Oct. 1996.
[24] D. Simunic, P. Wach, W. Renhart, and R. Stollberger, "Spatial distribution of high-frequency electromagnetic energy in human head during MRI: Numerical results and measurements," *IEEE Trans. Biomed. Eng.*, vol. 43, no. 1, p. 88, Jan. 1996.
[25] W. C. Dewey, D. E. Thrall, and E. L. Gillette, "Hyperthermia and radiation—Selective thermal effect on chronically hypoxic tumor-cells in vivo," *Int. J. Radiat. Oncol. Biol. Phys.*, vol. 2, p. 99, 1977.
[26] A. Hoshino, K. Fujioka, T. Oku, M. Suga, Y. F. Sasaki, T. Ohta, M. Yasuhara, K. Suzuki, and K. Yamamoto, "Physicochemical properties and cellular toxicity of nanocrystal quantum dots depend on their surface modification," *Nano Lett.*, vol. 4, p. 2163, 2004.

Manuscript received October 28, 2005; revised February 3, 2006. Corresponding author: S. Maenosono (e-mail: shinya@chemsys.t.u-tokyo.ac.jp).